Journal of the European Ceramic Society **19** (1999) 33–39

PII: S0955-2219(98)00174-5
0955-2219/98/$—see front matter

Optimizing Mechanical Properties and Thermal Stability of Ln-α-β-Sialon by Using Duplex Ln Elements (Dy and Sm)

C. Zhang, W. Y. Sun* and D. S. Yan

The State Key Lab on High Performance Ceramics and Superfine Microstructure, Shanghai Institute of Ceramics, Shanghai 200050, People's Republic of China

(Received 6 February 1998; accepted 6 July 1998)

Abstract

The densification behavior, phase transformation, microstructure and mechanical properties of α-β-*sialon ceramics have been compared among the counterpart Ln-*α-β-*sialon compositions where Ln represents Dy, Sm and (Dy + Sm). Sm-sialons have a rather finer microstructure, higher flexural strength and fracture toughness, but their hardness are relatively lower. Dy-sialons possess a higher hardness. Unlike Sm-sialon, Dy-sialons have kinetically priority in the formation of* α-*sialon over the other Dy-containing phases (such as melilite and garnet phases) thus giving a higher content of* α-*sialon than the designed value. Dy-*α-*sialon is much stable than Sm-*α-*sialon during heat treatment. The higher flexural strength and fracture toughness of Sm-sialons and the higher hardness and good stability of Dy-sialons can remain in the (Dy + Sm)-sialons.* © *1998 Elsevier Science Limited. All rights reserved*

Keywords: sialon, mechanical properties, thermal stability, microstructure-final, sintering

1 Introduction

In recent years Ln-sialon ceramics have attracted much attention. Not only can their mechanical properties be adjusted by varying the ratio of α-sialon(α') to β-sialon(β'), but also it provides the possibility to reduce the grain boundary glassy phase because the rare earth ions can be accommodated in α-sialon structure. The behavior of rare earth elements in the phase relationships in the Ln–Si–Al–O–N system, and their ability to form α-sialon vary with increasing Z-value of Ln elements.

*To whom correspondence should be addressed.

Samarium is a typical light rare earth element and its phase relationships with Si–Al–O–N is slightly different from those in the Y–Si–Al–O–N[1,2] and Dy–Si–Al–O–N systems.[3] In the Sm_2O_3–Si_3N_4–AlN–Al_2O_3 system,[4] $SmAlO_3$ and M′ phase (melilite solid solution, $Sm_2Si_{3-x}Al_xO_{3+x}N_{4-x}$, $x = 0 \rightarrow 1{\cdot}0$) are the only two important compounds which have tie lines joined to β-sialon and AlN polytypoid phases. M′ phase coexists with α-sialon. Samarium oxide with Al_2O_3 have been found to be a good sintering additives and many work on Sm-α-β-sialon has been carried out.[5] Besides, our current work on Sm-sialons indicated that the grain growth seems to be retarded and the finer microstructure might be the reason for giving a higher flexural strength. However, in the studies on $\alpha' \rightarrow \beta'$ phase transformation, the results obtained by the laboratories[6–9] all indicated that the Ln-α' with light Ln elements, such as Nd and Sm, is quite unstable during heat treatment. This disadvantage leads to poor reproducibility in controlling phase distribution during fabrication and also restricts their application at medium temperatures. Dysprosium is the one situated at the central position of the rare earth element series. Its phase relationships in the Dy–Si–Al–O–N system do exhibit some difference from Sm- and Y–Si–Al– O–N systems. In the Dy_2O_3–Si_3N_4–AlN–Al_2O_3 region,[3] DyAG (garnet phase, $Dy_3Al_5O_{12}$) and M′ phase are the only two compounds which have tie lines joined to β-sialon and AlN-polytypoids. α-Sialon coexists with both M′ phase and DyAG. The solubility region of Ln–α–sialon increases with the increasing Z-value of Ln elements, but for all Ln-α-sialon ($Ln_{1/3m}Si_{12-(m+n)}Al_{m+n}O_nN_{16-n}$), the minimum m value is 1·0.[10] Recently, the extension of α-sialon phase area was determined by many authors. The minimum m value of 1·0 for all Ln(Y)-α-sialon was further confirmed, but the maximum n value was reported to be different.

Shen *et al.*[11] indicated that n_{max} is ~1·0 for Nd and ~1·2 for the other Ln-doped α-sialon. Chen *et al.*[12] observed that the n_{max} is ~1·2 for Nd, ~1·6 for Y and ~1·8 for Yb, which are more close to the $n_{max} = 1{\cdot}7$ for Y-α-sialon previously reported.[2] The different results for the maximum n value was caused by experimental errors because the measurement for the light anions by using EDS is not so accurate as for heavy elements. However, it was confirmed that the maximum n value increases with the increasing Z-value of Ln elements. The solubility region of α-sialon phase seems also to be related with their formability. In the Sm-sialon, it has been observed that the formation of α-sialon is suppressed by the formation of M′. However, our recent work[10] on Dy-sialon ceramics showed that the formation of Dy-α' has a kinetic priority over the formation of M′ and DyAG, but the over-formed α' will transform into β' during heat treatment and then the phase composition can reach the equilibrium value. This is an important merit for α-β-sialon ceramics. The aim of the present work is to explore the possibility to tailor the properties and characteristic existing in Sm- and Dy-sialons through using the duplex Sm and Dy as α-sialon modification ions.

2 Experimental

Three series of compositions with Dy, Sm and Dy:Sm (1:1 in mole) as α-sialon modification ions were prepared. The ratio of α' to β' were fixed to be 100:0, 65:30 and 30:65 (in wt%) with extra 5 wt% sintering additives for the latter two compositions. The sintering additives used were Sm_2O_3 plus Al_2O_3 (corresponding to $SmAlO_3$) and Dy_2O_3 plus Al_2O_3 (corresponding to DyAG) for Sm- and Dy-compositions, and $SmAlO_3$ + DyAG (1:1 in weight) for (Dy + Sm)-compositions. Based on the phase relationships,[3] both DyAG and M′ can be used as grain boundary phases for Dy-α'-β' ceramics. Our current work on Dy-sialon indicated that as sintering additives, DyAG is more effective than M′. In order to compare the densification behavior among the different series, therefore, the lanthanide aluminates DyAG and $SmAlO_3$ (no garnet phase in the Sm–Si–Al–O–N system) were selected as sintering additives.

For the composition calculation of α-β-sialon ceramics, the α-sialon composition with m_{min} ($m = 1$) and n_{max} (the boundary facing to β') should be used. Sm-α-sialon has a smaller n_{max} than Dy-α-sialon, but for comparison the same value was used for all the compositions. Based on our previous work on Y-α-sialon, 1·7 was taken as the maximum n value, which is probably slightly larger than for Dy-doped α-sialon. Therefore, the composition $Ln_{0.33}Si_{9.3}Al_{2.7}O_{1.7}N_{14.3}$ (i.e. $m = 1$, $n = 1{\cdot}7$) for α' and $Si_{5.2}Al_{0.8}O_{0.8}N_{7.2}$ (i.e. $z = 0{\cdot}8$) for β' were assumed. The starting materials used were Si_3N_4 (UBE), AlN (1·2 wt% oxygen), Al_2O_3 (99·99%) and Ln_2O_3 (Ln = Dy, Sm, 99·9%, Yaolong Chemical Works). The oxygen contents of the nitride powders were taken into account in calculating the compositions. The starting powders, as listed in Table 1, were weighted and mixed with absolute alcohol by milling for 24 h with Si_3N_4 balls as media. The mixed powders were hot-pressed under 25 MPa, at 1800°C for 1 h in a graphite resistance furnace in N_2. The phases were analyzed by X-ray diffraction technique and the α'/β' ratio was estimated based on a calibration curve by using the diffraction peaks (210) for both α' and β'. The shrink curves were determined during hot-pressing with a raising speed of 15°C/min^{-1} (1400–1800°C). Hardness and indentation fracture toughness were measured by using a Vickers diamond indenter under a load of 100 N. Flexural strength was tested by three-point bending with a 20 mm span. Both polished and fracture surface were observed by SEM.

3 Results and Discussions

3.1 Densification behavior and phase transformation

All the compositions listed in Table 1 were fully densified through hot pressing at 1800°C for 1 h. For comparing the densification behavior among these three series, the shrinkage of the α'-β' compositions with 30% α'–65% β' (S-2, D-2 and DS-2) were determined (see Fig. 1). Obviously, the mixed additives ($Dy_2O_3 + Sm_2O_3$) with Al_2O_3 promote densification more effectively. As indicated in Fig. 1, the composition DS-2 starts to shrink at around 1350°C which is about 70–100°C below the corresponding temperatures for the compositions S-2 (1420°C) and D-2 (1450°C). Based on the knowledge of phase diagram, the eutectic temperature will further decrease by adding extra element.

Table 1. Starting compositions of the specimens (wt%)

No.	Dy_2O_3	Sm_2O_3	Si_3N_4	*AlN*	Al_2O_3
D-0	10·00		71·27	15·07	3·66
D-1	9·94		72·59	11·82	5·66
D-2	6·44		78·30	8·88	6·37
S-0		9·94	72·59	11·82	5·66
S-1		10·13	73·64	11·92	4·31
S-2		6·44	78·30	8·88	6·37
DS-0	5·04	4·96	71·27	15·07	3·66
DS-1	5·21	5·17	71·98	11·78	5·86
DS-2	3·53	3·50	77·61	8·84	6·52

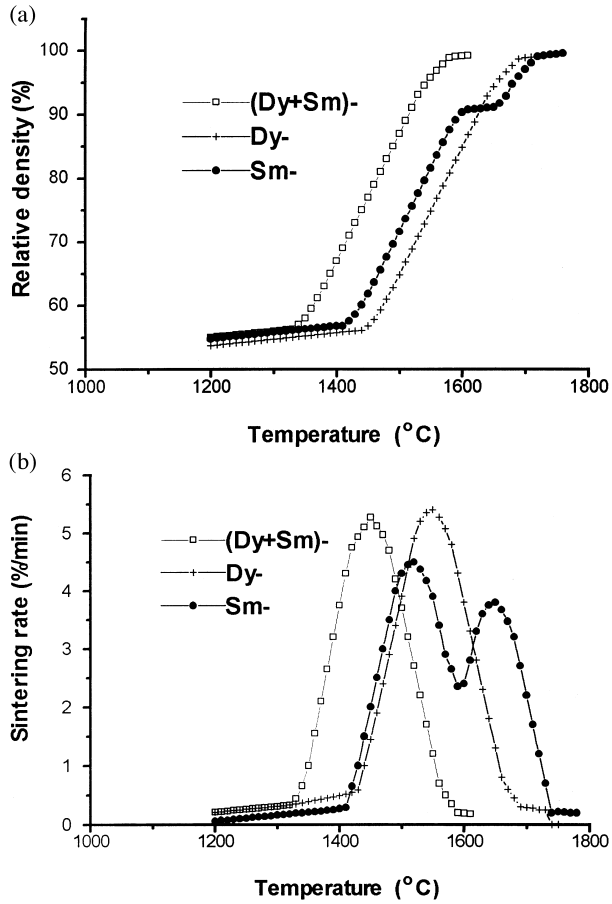

Fig. 1. The densification behavior of the counterpart compositions D-2, S-2 and DS-2, (a) represented by relative density; (b) represented by shrinkage rate.

Therefore, the (Dy + Sm)-sialon should have the lowest eutectic temperature among these three sialon systems. In Sm-sialon, it was observed that M′ phase always occurs accompanied with the formation of α-sialon.[5] The occurrence of M′ phase which starts at around 1550°C[13] retards the densification progress because it exhausts the liquid phase in the compositions. With the temperature increasing and the preformed melilite dissolving, the densification progress can be restored. This is in good agreement with the shrinkage behavior of the Sm-sialon composition which shows a critical point around 1550–1600°C. The addition of Dy into the Sm-sialons suppresses the formation of M′, therefore, as indicated in Fig. 1, no critical point occurs in the densification progress.

The phase compositions designed and as fired are summarized in Table 2. As indicated, the α′ formed in the Dy-sialon is larger than the designed value. This is consistent with our other work on Dy-sialon ceramics where the α-sialon content is always higher than it should be, even in the β′-DyAG compositions where small amount of α′ also occurs, but during heat treatment, the over-formed α-sialon will transform into β′ and then reaches the equilibrium.[14] However, in the Sm-sialons the situation goes opposite, i.e. less α′ is formed than

Table 2. Phase compositions designed and observed after H.P. at 1800°C for 1 h

No.	*Phase compositions designed*				*Phase compositions observed*		
	α′	β′	*DyAG*	*SAO*[a]	α′	β′	*G.B. phase*
D-0	100				90	10	—
D-1	65	30	5·0		85	15	—
D-2	30	65	5·0		50	50	—
S-0	100				85	15	M′ w
S-1	65	30		5·0	50	50	M′ w
S-2	30	65		5·0	20	80	M′ w
DS-0	100				95	5	—
DS-1	65	30	2·5	2·5	70	30	—
DS-2	30	65	2·5	2·5	30	70	—

[a]SAO: $SmAlO_3$.

the designed. As indicated in Table 2, during cooling down with the furnace, no crystalline grain boundary phase was observed in all the compositions, except in Sm-compositions where small amount of M′ exists. This might be a reason for the less content of α′ in the Sm-sialons. In the (Dy + Sm)-sialons, the as fired α′/β′ is very close to the designed value. Obviously, the formation of α′ in Dy-sialon system has kinetic priority over the other Dy-containing phase, but this kinetic priority diminishes with the addition of Sm. In the single phase Dy-containing α-sialon compositions (D-0, SD-0), where no Dy-containing phase was observed after sintering, the occurrence of β-sialon can be attributed to the existence of unavoidable glassy phase, which, like M′, also exhausts the Ln content in the compositions.

The phase compositions after heat treatment (1450°C for 72 h) are compared in Table 3. As indicated, the α′→β′ phase transformation occurs in all the compositions, but the transformable quantity is different. In the Dy-sialons, the over-formed α′ seems to completely transform into β′ through heat treatment and then the designed value can be achieved. In the Sm-sialons, as observed in other previous work,[6–9] the transformable α′ is

Table 3. Phase compositions after H.T. at 1450°C for 72 h

No.	*Phase compositions as fired*					*Phase composition after H.T.*				
	α′	β′	*DyAG*	*SAO*	*M′*	α′	β′	*DyAG*	*SAO*	*M′*
D-0	90	10								
D-1	85	15				65	35	w		
D-2	50	50				30	70	w		
S-0	85	15			w	70	30			m
S-1	50	50			w	30	70		w	m
S-2	20	80			w	5	95		w	m
DS-0	95	5				90	10	vw		
DS-1	70	30				60	40	w	w	vw
DS-2	30	70				20	80	w	w	vw

quite large. The $\alpha' \rightarrow \beta'$ phase transformation in the (Dy + Sm)-sialons is less than in the Sm-sialons. For clearly showing these variation, the designed, as fired and heat treated values for these three series with the composition of 65% α'–30% β'(D-1, S-1 and DS-1) are compared in Fig. 2. As shown, the α' content in the Sm-sialon decreases all the way from left (designed) to right column (heat treated). However, the variation of α'/β' ratio in the (Dy + Sm)-sialon is very slight. Therefore, the merit of (Dy + Sm)-sialon in this aspect is obvious because keeping the consistence of α'/β' ratio from design, fabrication until application at medium temperature is of the most importance for α-β-sialon ceramics. The mechanism of $\alpha' \rightarrow \beta'$ phase transformation has been widely reported in the literature,[6–8] but there still left some points in argument. In the Sm-sialon compositions, besides the intrinsic properties of Sm-α', the kinetic priority of the formation of Sm-M′ is an extrinsic factor for promoting the $\alpha' \rightarrow \beta'$ phase transformation because the crystallization of melilite during heat treatment competes with α-sialon for Sm. However, with the increasing Z value of the Ln elements, the diminishing tendency in the formation of melilite at least extrinsically reduces the drawing force for the $\alpha' \rightarrow \beta'$ phase transformation. In the Ln-sialons with mixed light and heavy rare-earth elements, such as Sm plus Dy, the light Ln-α' seems to become more stable. Obviously, this is a good approach to stabilize Sm(or Nd)-α'.

3.2 Mechanical properties and microstructure

The mechanical properties observed are represented in Figs 3–5 showing the flexural strength, hardness and fracture toughness varying with the measured α' content. As indicated, with increasing α' content, the flexural strength and fracture toughness decrease, and the hardness increase because β' possesses higher flexural strength and fracture toughness and α' has good hardness. The difference in mechanical properties in the counterpart compositions is obvious. As indicated, the Sm-sialons possess the highest flexural strength with a value of 810 MPa (actually containing 85% α') to 870 MPa (20% α'). The flexural strength of (Dy + Sm)-sialons are very close to those of Sm-sialons; they vary from 770 MPa (95% α') to

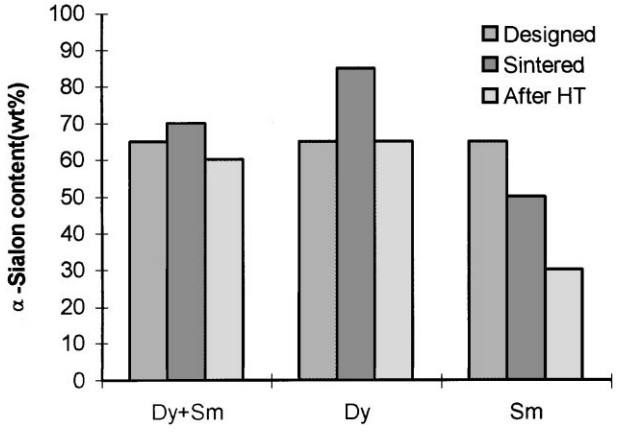

Fig. 2. The variation of α'/β' ratio during different stages in the compositions D-1, S-1 and DS-1.

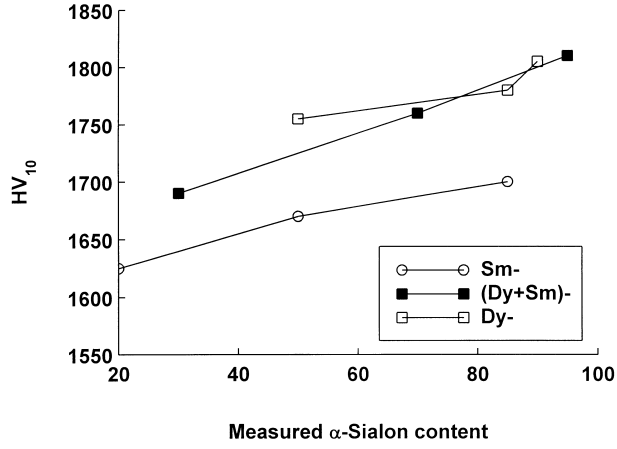

Fig. 4. The hardness of the compositions hot pressed at 1800°C for 1 h versus α' content.

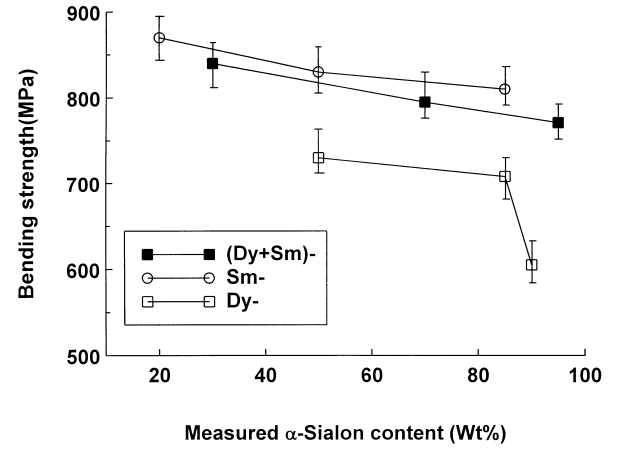

Fig. 3. The flexural strength of the compositions hot pressed at 1800°C for 1 h versus α' content.

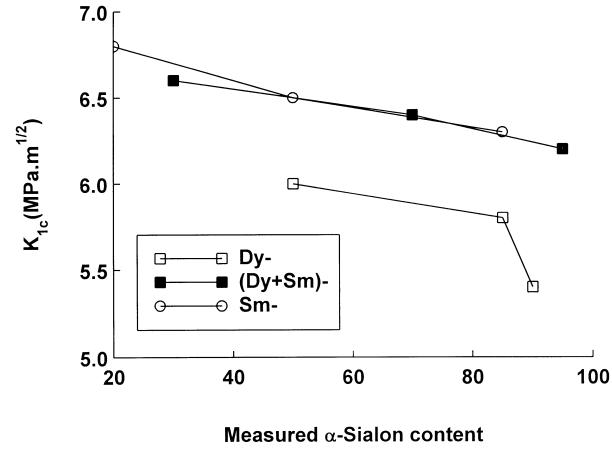

Fig. 5. The fraction toughness of the compositions hot pressed at 1800°C for 1 h versus α' content.

840 MPa (30% α'). The Dy-sialons have the lowest flexural strength. However, in the hardness, the Dy-sialons exhibit the highest value varying from 1755 to 1805 (HV_{10}). The (Dy + Sm)-sialons, especially with high α' content, possess a similar hardness to the Dy-sialons. The variation of K_{1c} with Ln elements behaves in a similar way to that of flexural strength. Sm-sialons and Dy-sialons

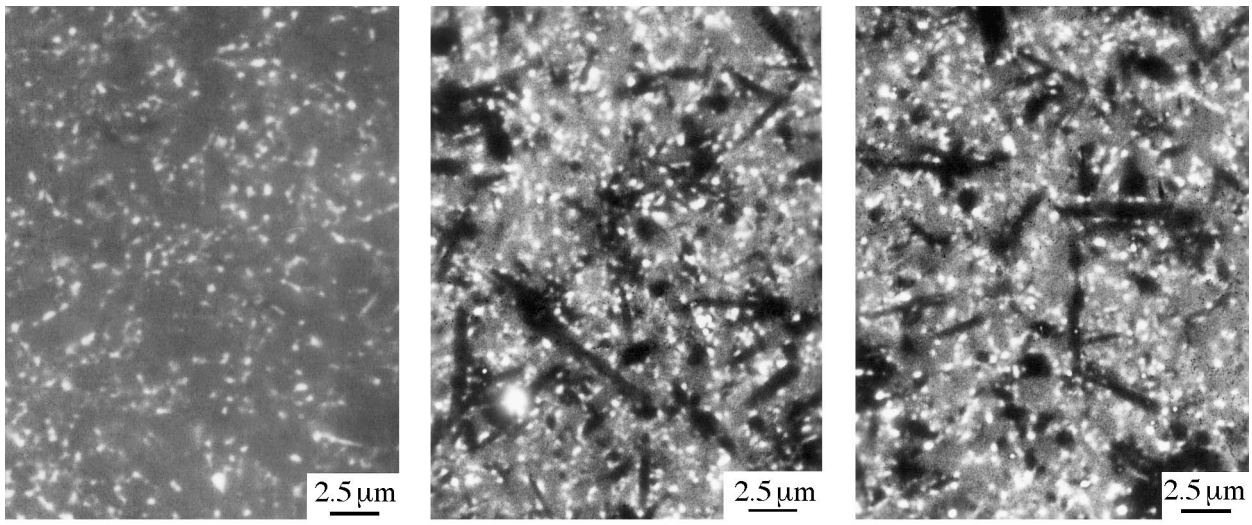

Fig. 6. SEM micrographs (back-scattered mode) of the compositions hot pressed at 1800°C for 1 h: (a) D-1, (b) S-1 and (c) DS-1.

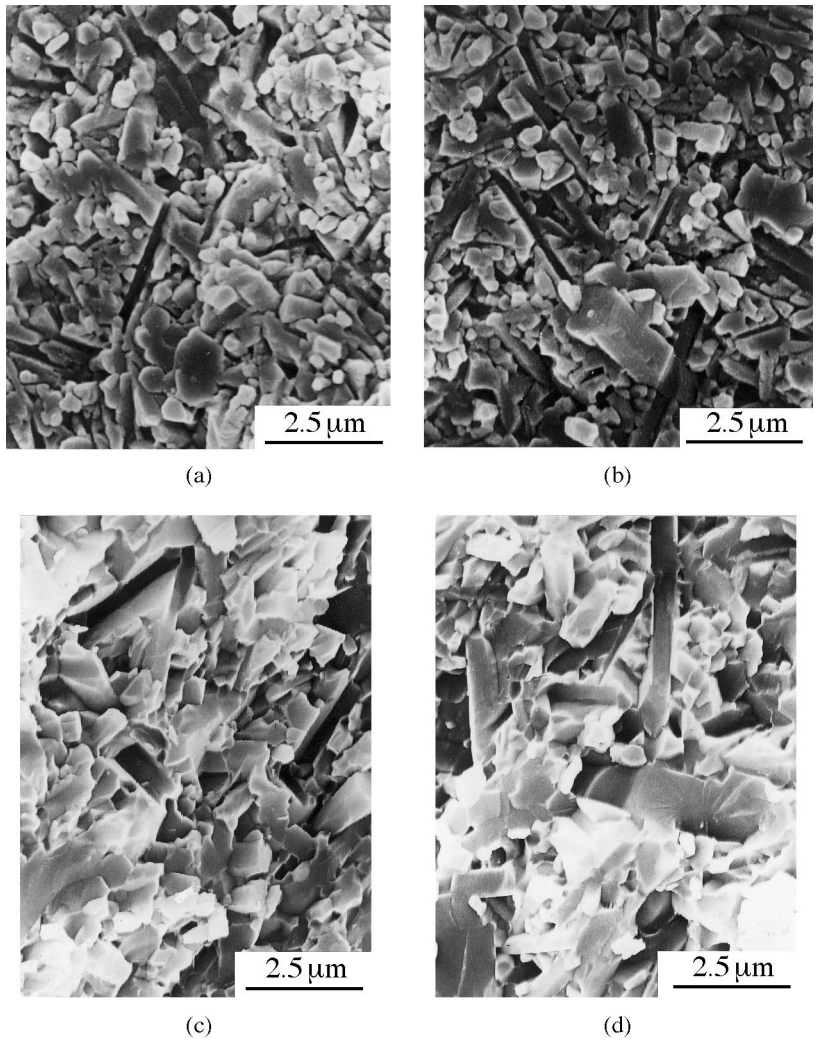

Fig. 7. The SEM photos of fracture surface of the compositions hot-pressed at 1800°C for 1 h: (a) S-1, (b) S-2, (c) DS-1 and (d) DS-2.

exhibit the highest and the lowest K_{1c}, respectively, and the K_{1c} of (Dy + Sm)-sialons are very close to Sm-sialons. Based on the above data, obviously, besides the thermal stability, the mechanical properties of the Ln-sialon ceramics can also be improved or tailored by using duplex Ln elements. As indicated in the present work, the Ln-sialons with mixed light and heavy rare earth elements, such as Sm and Dy, will have a best combination of mechanical properties.

The variation of mechanical properties of Ln-α-β-sialons with Ln elements, besides their phase compositions, must have some relevance with their microstructures.[15] Figure 6 shows the back-scatted SEM micrographs of the α-β-sialon with 65α'–30β' (D-1, S-1 and DS-1), where grain boundary phases are bright, α' grains are grey and β' are black because the glassy phases contain more Ln than α' and no Ln in β'. As indicated, the amount of β' in the composition D-1 is quite small, which is in consistent with indicated by X-ray analysis (15% β'), and no needle-like β' grains was observed. However, in the compositions S-1 (50% β') and DS-1 (30% β'), most of the β' grains develop into needle-like with similar morphology. The slight difference between Sm- and (Dy + Sm)-sialons can be clearly seen in the fracture morphology. Figure 7 shows the fracture surface of the compositions S-1, S-2, DS-1 and DS-2. As indicated, the long β-sialon grains and the pull-out cavitations can be clearly observed. In comparison, the grains in the (Dy + Sm)-sialons are slightly bigger than those in the Sm-sialons. Based on these SEM photos (Figs 6 and 7), it can be concluded that the microstructural characteristic of Sm-sialons can still remain in the (Dy + Sm)-sialon. The small grain size with higher aspect ratio of β' in the Sm-sialons must have some effect to contribute to the higher flexural strength and fracture toughness. It has been generally accepted that the hardness increases with the amount of α-sialon present because of longer Burgers vector in the structure of α-Si_3N_4 (or α-sialon). Besides the α-sialon content, the hardness of α'–β' ceramics is relevant to the amount and compositions of grain boundary phases, and other factors, such as density, microcracks. The compositions D-1 (actually containing 85% α') and D-2 (50% α') contain the same amount of α' with the compositions S-0 (85% α') and S-1 (50% α'), respectively, but the Dy-compositions have higher hardness than Sm-compositions. The small grain size and the more grain boundary glassy phase might be the main reason for the lower hardness in the Sm-sialons. In the present work, the fraction of glassy phase in the compositions could not been determined, but it can be assumed that in the counterpart compositions, the Sm-sialons contain more glassy phase because the less formation of α' must leave some of Sm in the liquid phase.

4 Conclusion

1. The (Dy + Sm)-sialons are more easy to be densified than the counterpart Dy- and Sm-compositions. On the shrinkage curve of Sm-sialons, there exists a critical point at 1550–1600°C which corresponds to the temperature of forming Sm-melilite.
2. In the Dy-sialons, the as fired α'/β' is higher than the designed value and vice versa in the Sm-sialons. During heat treatment, the over-formed Dy-α' completely transforms into β' and then achieving the designed value. In the (Dy + Sm)-sialon, the as fired α'/β' is very closed to the designed and only slightly decreases during heat treatment.
3. The Sm-sialons possess the highest flexural strength (810–870 MPa) and fracture toughness (6·3–6·8 MPa $m^{1/2}$) and Dy-sialons have rather higher hardness. The good mechanical properties exhibiting in both Sm- and Dy-sialons can remain in the (Dy + Sm)-sialons.
4. The Sm-sialons possess rather fine microstructure with needle-like β' grains mixed with α' grains, but the morphology of the Dy-sialons is relatively coarse and no needle-like β' grains was observed. The morphology characteristic of Sm-sialons can remain in the (Dy + Sm)-sialons.

Acknowledgement

This work has received financial support from the National Natural Science Foundation of China, contract no. 59632100.

References

1. Sun, W. Y., Tien, T. Y. and Yan, D. S., Subsolidus phase relationships in part of the system Si,Al,Y/N,O: the system Si_3N_4–AlN–YN–Al_2O_3–Y_2O_3. *J. Am. Ceram. Soc.*, 1991, **74**, 2753–2758.
2. Sun, W. Y., Tien, T. Y. and Yan, D. S., Solubility limits of α-SiAlON solid solutions in the system Si,Al,Y/N,O. *J. Am. Ceram. Soc.*, 1991, **75**, 2547–2550.
3. Sun, W. Y., Yan, D. S., Guo, L., Mandal, H. and Thompson, D. P., Subsolidus phase relationships in the systems Dy_2O_3–Si_3N_4–AlN–Al_2O_3. *Journal of the European Ceramic Society*, 1996, **16**, 1277–1282.
4. Sun, W. Y., Yan, D. S., Guo, L., Mandal, H., Liddell, K. and Thompson, D. P., Subsolidus phase relationships in the system Ln_2O_3–Si_3N_4–AlN–Al_2O_3 (Ln = Nd,Sm). *Journal of the European Ceramic Society*, 1995, **15**, 349–355.
5. Cheng, Y. B. and Thompson, D. P., Preparation and grain boundary devitrification of samarium α-sialon

ceramics. *Journal of the European Ceramic Society*, 1994, **14**, 13–21.
6. Sun, W. Y., Wang, P. L. and Yan, D. S., The $\alpha' \rightarrow \beta'$ phase transformation in sialon ceramics by heat treatment. *Mater. Lett*., 1996, **26**, 9–16.
7. Shen, Z. J., Ekstrom, T. and Nygren, M., Temperature stability of samarium doped α-sialon ceramics. *Journal of the European Ceramic Society*, 1996, **16**, 43–53.
8. Zhao, R. P. and Cheng, Y.-B., Phase transformations in Sm($\alpha + \beta$)-sialon ceramics during post-sintering heat treatment. *Journal of the European Ceramic Society*, 1996, **16**, 1001–1008.
9. Ekstrom, T., Falk Lena, K. L. and Shen, Z. J., Duplex α-β-sialon ceramics stabilized by dysprosium samarium. *J. Am. Ceram. Soc*., 1997, **80**, 301–312.
10. Huang, Z. K., Tien, T. Y. and Yen, T. S., Subsolidus phase relationships in Si_3N_4–AlN–rare earth oxide systems. *J. Am. Ceram. Soc*., 1986, **69**, C241–C242.
11. Shen, Z. J. and Nygren, M., On the extension of α-sialon phase area in yttrium and rare-earth doped systems. *Journal of the European Ceramic Society*, 1997, **17**, 1639–1645.
12. Chen, I-.W. and Rosenflanz, A., A tough SiAlON ceramic based on α-Si_3N_4 with a whisker-like microstructure. *Nature*, 1997, **389**, 701–704.
13. Wang, P. L., Tu, H. Y., Sun, W. Y., Yan, D. S., Nygren, M. and Ekstrom, T., Study on the solid solubility of Al in the melilite systems $R_2Si_{3-x}Al_xO_{3+x}N_{4-x}$ with R = Nd, Sm, Gd and Y. *Journal of the European Ceramic Society*, 1995, **15**, 689–695.
14. Sun, W. Y., Chen, H. G. and Yan, D. S., Kinetic study on β-sialon-DyAG ceramics. *Mater. Sci. Lett*, 1997, **16**, 1853–1855.
15. Sheu, T. S., Microstructure and mechanical properties of the in situ β-Si_3N_4/α-SiAlON composite. *J. Am. Ceram. Soc*., 1994, **77**, 2545–2553.